Linearly independent pure-state decomposition and quantum state discrimination

Luis Roa, M. Alid-Vaccarezza, and A. Maldonado-Trapp
Departamento de Física, Universidad de Concepción, Concepción, Chile
(Received 3 November 2010; revised manuscript received 5 May 2011; published 18 August 2011)

We put the pure-state decomposition mathematical property of a mixed state to a physical test. We present a protocol for preparing two known nonorthogonal quantum states with well-defined *a priori* probabilities. Hence we characterize all the possible decompositions of a rank-two mixed state by means of the complex overlap between the two involved states. The physical test proposes a scheme for quantum state recognition of one of the two linearly independent states that arise from the decomposition. We find that the two states associated with the balanced pure-state decomposition have the smaller overlap modulus and therefore the smallest probability of being discriminated conclusively, while in the nonconclusive process they have the highest probability of having an error. In addition, we design an experimental scheme that allows discriminating conclusively and optimally two nonorthogonal states prepared with different *a priori* probabilities. Thus we propose a physical implementation for this linearly independent pure-state decomposition and state discrimination test by using twin photons generated in the process of spontaneous parametric down-conversion. The information state is encoded in a one-photon polarization state, whereas the second single photon is used for heralded detection.

DOI: 10.1103/PhysRevA.84.022110 PACS number(s): 03.65.Ta, 42.50.Dv

I. INTRODUCTION

In quantum information and computation, the physical unit for storing and processing information is a microscopic system, and the information itself is encoded in its quantum state [1]. If the system is isolated, all its properties are described by a pure state. The fundamental property of a pure state is that it always can be expressed as a coherent superposition of linearly independent states, which, for instance, gives an account of the accurate quantum interference phenomenon [2]. If the system is not isolated then, in general, it is correlated with an uncontrollable quantum system, usually called environment, which introduces decoherence into the state of the system [3]. In this case, the effective state of the system can be described by a mixed state, which consists of an incoherent superposition of possible states. In addition, a partial knowledge of the state of a system that belongs to a reservoir also is required to be effectively described by a mixed state. Whatever the cause for the mixture, it has the fundamental property of having an infinite number of decompositions. There are some properties that do not depend on the considered decomposition, for instance, eigenvalues, eigenstates, observable-average, purity, and entropy. However, some others, like the average entanglement for a bipartite mixed state, do depend on it. The entanglement of formation is defined to be the least average entanglement, minimized over all possible pure-state decompositions [4].

On the other hand, a nonorthogonal quantum state discrimination protocol makes use of a mixed composition of the possible prepared states averaged over their *a priori* probabilities. We find below that the process of preparing two nonorthogonal states commutes with the process of discriminating which of the two states was prepared. Therefore, the set of nonorthogonal states could be chosen from any one decomposition of the mixed state. The property of commuting those processes could be used as a new strategy for performing secure quantum cryptography.

In this way, the mathematical-decomposition property is a nonclassical characteristic [4,5] and becomes of fundamental physical interest.

In this paper, we relate the linearly independent (LI) pure-state decomposition property of a given mixed state to the unambiguous quantum state discrimination (UQSD) [6–10] protocol and to the strategy of allowing a minimum-error tolerance of discriminating the state [11–13]. In the simplest case, the state is in a two-dimensional Hilbert space and only two different states are LI. In a Hilbert space with dimension higher than two, the states require additional constraints to be LI [14]. In order to simplify the study of the addressed problem, we have considered a rank-two mixed state.

In Sec. II, we propose a protocol for preparing a qubit in two nonorthogonal states by starting from an entangled pure state. In Sec. III, we characterize all the possible decompositions of a rank-two mixed state by means of the complex overlap between the two involved states. In Sec. IV, we study the optimal success probability for quantum state recognition of one of the two linearly independent states that arise from the decomposition. In Sec. V, we propose an optical setup for implementing conclusive nonorthogonal-state discriminations that have been prepared with different *a priori* probabilities. Finally, in the last section, we resume our main results.

II. NONORTHOGONAL-STATE PREPARATION

Recently, the mapping between sets of nonorthogonal states has been connected to the control of quantum state preparation [15]. In this section, we describe a protocol for preparing two known nonorthogonal pure states with well-defined *a priori* probabilities. Let us consider a physical setup, which can generate a known entangled pure state $|\Omega\rangle_{AB}$ of two qubits A and B. In its Schmidt representation, that state is read as

$$|\Omega\rangle_{AB} = \sqrt{\lambda_1}|\lambda_1\rangle_A|u_1\rangle_B + \sqrt{\lambda_2}|\lambda_2\rangle_A|u_2\rangle_B, \qquad (1)$$

where $\{|\lambda_1\rangle_A,|\lambda_2\rangle_A\}$ and $\{|u_1\rangle_B,|u_2\rangle_B\}$ are the respective orthonormal Schmidt bases [1], with $\lambda_1 + \lambda_2 = 1$. We expand each state $|u_1\rangle_B$ and $|u_2\rangle_B$ on another orthonormal basis

$\{|v_1\rangle_B, |v_2\rangle_B\}$ according to

$$|u_1\rangle_B = y|v_1\rangle_B + \sqrt{1-y^2}|v_2\rangle_B, \tag{2a}$$

$$|u_2\rangle_B = \sqrt{1-y^2}|v_1\rangle_B - y|v_2\rangle_B, \tag{2b}$$

where $y = \langle v_1|u_1\rangle$ is a probability amplitude assumed to be a real number and $-1 \leqslant y \leqslant 1$. Inserting the Eq. (2) states into Eq. (1) we obtain, in this way, another representation of the $|\Omega\rangle_{AB}$ state,

$$|\Omega\rangle_{AB} = \sqrt{p_1}|\beta_1\rangle_A|v_1\rangle_B + \sqrt{p_2}|\beta_2\rangle_A|v_2\rangle_B. \tag{3}$$

Here we have defined the nonorthogonal states,

$$|\beta_1\rangle_A = \frac{y\sqrt{\lambda_1}|\lambda_1\rangle_A + \sqrt{1-y^2}\sqrt{\lambda_2}|\lambda_2\rangle_A}{\sqrt{p_1}},$$

$$|\beta_2\rangle_A = \frac{\sqrt{1-y^2}\sqrt{\lambda_1}|\lambda_1\rangle_A - y\sqrt{\lambda_1}|\lambda_2\rangle_A}{\sqrt{p_2}},$$

and the complementary probabilities,

$$p_1 = 1 - p_2 = y^2\lambda_1 + (1-y^2)\lambda_2. \tag{4}$$

The $|\Omega\rangle_{AB}$ state in the Eq. (3) representation is expanded in an orthonormal basis $\{|v_1\rangle_B, |v_2\rangle_B\}$ of the B subsystem and in a nonorthogonal basis $\{|\beta_i\rangle_A\}$ of the A subsystem, having also a one-to-one correspondence between those states, similar to the Schmidt representation (1). By performing a von Neumann measurement on the basis $\{|v_i\rangle_B\}$ of the B subsystem, we also project the A subsystem onto $|\beta_1\rangle_A$ with probability p_1 or onto $|\beta_2\rangle_A$ with probability p_2. In this way, after choosing the $\{|v_i\rangle_B\}$ orthogonal basis, the respective nonorthogonal states $\{|\beta_i\rangle_A\}$ are prepared with the *a priori* probabilities p_i. In other words, the $\{|\beta_i\rangle_A, p_i\}$ state preparation is performed via a von Neumann measurement on the basis $\{|v_i\rangle_B\}$. The so prepared states $\{|\beta_i\rangle_A, p_i\}$ can be used for any quantum information protocol. For instance, quantum cryptography, conclusive state discrimination, minimal-error state estimation, and quantum tomography [16], among others.

Notice that it is possible to commute the process of state preparation (project onto $\{|v_i\rangle_B\}$) with the unambiguous state discrimination process ($\{|\beta_i\rangle_A\}$), because of the one-to-one correspondence between those states. If, in the preparation, the B system is projected onto $\{|v_1\rangle_B\}$ ($\{|v_2\rangle_B\}$), then with some probability of success the $\{|\beta_1\rangle_A\}$ ($\{|\beta_2\rangle_A\}$) can be recognized in the A system. Otherwise, if with a certain probability of success the $\{|\beta_1\rangle_A\}$ ($\{|\beta_2\rangle_A\}$) is recognized in the A system, then the B system shall be in $\{|v_1\rangle_B\}$ ($\{|v_2\rangle_B\}$) with certainty. We realize that in the latter procedure the set $\{|\beta_i\rangle_A\}$ can be chosen from a wide family of sets, each one characterized by the parameter y. By communicating from A to B the chosen value of y when the UQSD process is successful, in the place where B is, one will know with certainty which state was recognized for A by measuring on the respective basis $\{|v_i\rangle_B\}$; see Eqs. (2).

III. MIXED-STATE DECOMPOSITION

Let us assume that the state of the A system is prepared as described above and, in addition, that the A and B systems are far away from each other. This means that only local operations on the A system are allowed. In this way, we can consider that the A system is in a mixed state whose known spectral decomposition is given by

$$\rho = \lambda_1|\lambda_1\rangle\langle\lambda_1| + \lambda_2|\lambda_2\rangle\langle\lambda_2|. \tag{5}$$

We omit the subscript A for simplifying the notation. In what follows, we shall assume λ_1 or λ_2 to be different from zero. Here we introduce two nonorthogonal states $|\beta_1\rangle$ and $|\beta_2\rangle$ with inner product $\langle\beta_1|\beta_2\rangle = \beta$. In terms of these states and of their biorthogonal ones [16,17], the identity can be represented as follows:

$$I = \frac{|\beta_1\rangle - \beta^*|\beta_2\rangle}{1-|\beta|^2}\langle\beta_1| + \frac{|\beta_2\rangle - \beta|\beta_1\rangle}{1-|\beta|^2}\langle\beta_2|. \tag{6}$$

This expression becomes the well-known canonical one for $\beta = 0$. Similarly to the trace onto an orthogonal basis, on the $\{|\beta_i\rangle\}|$ basis we get $\langle\beta_1|\rho|\beta_1\rangle + \langle\beta_2|\rho|\beta_2\rangle = 1 + |\langle\beta_1|\beta_2\rangle|^2$. This means that, by implementing statistical measurement procedures, we obtain the overlap modulus between the states of the considered decomposition. Making use of the Eq. (6) identity, we can find all possible decompositions of ρ whose forms are

$$\rho = p_1|\beta_1\rangle\langle\beta_1| + p_2|\beta_2\rangle\langle\beta_2|. \tag{7}$$

Here p_1 and p_2 play the role of the *a priori* probabilities associated with the $|\beta_1\rangle$ and $|\beta_2\rangle$ states, respectively. After some algebra, we obtain

$$p_1 = 1 - p_2 = \frac{\lambda_1\lambda_2}{\lambda_1 + (\lambda_2 - \lambda_1)|\gamma|^2}, \tag{8}$$

with $\gamma = |\gamma|e^{i\theta} = \langle\lambda_1|\beta_1\rangle$. p_1 as a function of $|\gamma|$ is monotonically increasing (for $\lambda_1 < \lambda_2$) or decreasing (for $\lambda_1 > \lambda_2$) and enclosed by λ_1 and λ_2.

We call that set $\{|\beta_i\rangle, p_i\}$ the $|\gamma|$ decomposition with

$$|\beta_1\rangle = \gamma|\lambda_1\rangle + \sqrt{1-|\gamma|^2}|\lambda_2\rangle, \tag{9a}$$

$$|\beta_2\rangle = \frac{\lambda_1\sqrt{1-|\gamma|^2}|\lambda_1\rangle - \lambda_2\gamma^*|\lambda_2\rangle}{\sqrt{\lambda_1^2 + (\lambda_2 - \lambda_1)|\gamma|^2}}, \tag{9b}$$

where the physical parameter $|\gamma|$ characterizes each possible decomposition. We point out that $\gamma = y\sqrt{\lambda_1}/\sqrt{y^2(\lambda_1 - \lambda_2) + \lambda_2}$ is related to the y parameter of the state preparation described in Sec. II.

From the Eq. (9) expressions we realize that the inner product between the allowed $\{|\beta_i\rangle\}$-decomposition states is given by

$$\langle\beta_1|\beta_2\rangle = \frac{(\lambda_1 - \lambda_2)|\gamma|\sqrt{1-|\gamma|^2}}{\sqrt{\lambda_1^2 + (\lambda_2 - \lambda_1)|\gamma|^2}}e^{-i\theta}. \tag{10}$$

We notice that, as is evident, when $\lambda_1 = \lambda_2$ all the possible decompositions are one-half of the identity since, in this case, we get $p_1 = p_2$ and all the possible sets $\{|\beta_i\rangle\}$ are orthonormal. From now on, we assume $\lambda_1 \neq \lambda_2$. On the other hand, the Eq. (5) spectral decomposition is recovered for both values $|\gamma| = 1$ and $|\gamma| = 0$.

The overlap modulus $|\beta|$ is a convex function of $|\gamma|^2$, being zero for $|\gamma| = 0$ and 1, and its maximum value is reached for

$$|\gamma| = \sqrt{\lambda_1}. \tag{11}$$

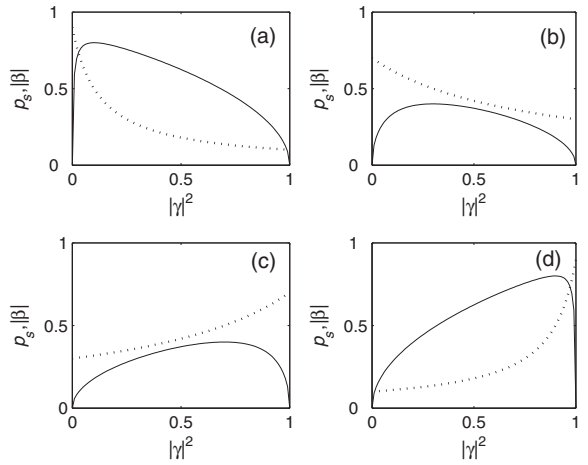

FIG. 1. $|\beta|$ (solid line) and *a priori* probability p_1 (dotted line) as functions of $|\gamma|^2$ for different values of λ_1: (a) $\lambda_1 = 0.1$, (b) $\lambda_1 = 0.3$, (c) $\lambda_1 = 0.7$, and (d) $\lambda_1 = 0.9$.

In this case, the decomposition corresponds to the *balanced* one, since $p_1 = p_2 = 1/2$ and the states become

$$|\beta_1\rangle = \sqrt{\lambda_1}e^{i\theta}|\lambda_1\rangle + \sqrt{\lambda_2}|\lambda_2\rangle, \tag{12a}$$

$$|\beta_2\rangle = \sqrt{\lambda_1}|\lambda_1\rangle - \sqrt{\lambda_2}e^{-i\theta}|\lambda_2\rangle, \tag{12b}$$

whose overlap is

$$\langle\beta_1|\beta_2\rangle = (\lambda_1 - \lambda_2)e^{-i\theta}. \tag{13}$$

Thus the balanced-decomposition states have the maximal modulus of the $\langle\beta_1|\beta_2\rangle$ overlap. In other words, in that decomposition, the two states $\{|\beta_i\rangle\}$ are as close as possible. Figure 1 illustrates those characteristics: the overlap modulus $|\beta|$ (solid) and the p_1 probability (dots) are shown as functions of $|\gamma|^2$ for different values of λ_1. Notice that p_1 is between λ_1 and λ_2 and $|\beta|$ reaches its maximal value at $|\gamma| = \sqrt{\lambda_1}$.

In this section, we have characterized by means of the parameter $|\gamma| = |\langle\beta_1|\lambda_1\rangle|$ all possible pure-state decompositions (7) of a given two-rank mixed state (5). The modulus of the overlap between the states of the decomposition goes from zero for the spectral decomposition up to $|\lambda_1 - \lambda_2|$ for the balanced decomposition, whereas its phase is $-\theta$ when $\lambda_1 > \lambda_2$ or $-\theta + \pi$ when $\lambda_1 < \lambda_2$. In the next section, we relate a possible $|\gamma|$ decomposition of a given density operator to the process for unambiguous nonorthogonal quantum state discrimination.

IV. QUANTUM STATE DISCRIMINATION

Dieks, Ivanovic, and Peres [7,19,20] addressed the fundamental problem of discriminating conclusively and without ambiguity two nonorthogonal states, $|\beta_1\rangle$ and $|\beta_2\rangle$, which are randomly prepared in a quantum system with *a priori* probabilities p_1 and p_2, respectively. The optimal success probability for removing the doubt as to which $|\beta_1\rangle$ or $|\beta_2\rangle$ the system is in was derived by Peres [7], Jeager, and Shimony [21], who obtained the expressions

$$p_s = 1 - 2\sqrt{p_1 p_2}|\beta|, \tag{14}$$

when $|\beta| \in [0, \min\{\sqrt{p_1/p_2}, \sqrt{p_2/p_1}\}]$, and

$$p_s = (1 - |\beta|^2)\max\{p_1, p_2\}, \tag{15}$$

when $|\beta| \in [\min\{\sqrt{p_1/p_2}, \sqrt{p_2/p_1}\}, 1]$. Inserting into these formulas both p_1 and p_2 from Eqs. (8) and $|\beta|$ from Eq. (10), we obtain the optimal probability of success for discriminating unambiguously the two nonorthogonal states of the $|\gamma|$ decomposition of a given ρ mixed state:

$$p_s = \begin{cases} 1 - 2\frac{|\lambda_1-\lambda_2||\gamma|\sqrt{\lambda_1\lambda_2(1-|\gamma|^2)}}{\lambda_1+(\lambda_2-\lambda_1)|\gamma|^2} & \text{if} \quad 0 \leqslant |\beta| \leqslant \min\left\{\sqrt{\frac{p_1}{p_2}}, \sqrt{\frac{p_2}{p_1}}\right\}, \\ \left(1 - \frac{|\lambda_1-\lambda_2|^2|\gamma|^2(1-|\gamma|^2)}{\lambda_1^2+(\lambda_2-\lambda_1)|\gamma|^2}\right)\frac{\max\{\lambda_1\lambda_2, \lambda_1^2+(\lambda_2-\lambda_1)|\gamma|^2\}}{\lambda_1+(\lambda_2-\lambda_1)|\gamma|^2} & \text{if} \quad \min\left\{\sqrt{\frac{p_1}{p_2}}, \sqrt{\frac{p_2}{p_1}}\right\} \leqslant |\beta| \leqslant 1. \end{cases} \tag{16}$$

As we know, for a given λ_1, the optimal probability p_s takes its highest value, 1, for the extreme values $|\gamma| = 0$, 1 that correspond to the spectral decomposition, whereas it reaches the smallest value just for $|\gamma| = \sqrt{\lambda_1}$, which corresponds to the balanced decomposition. In other words, the states belonging to the balanced decomposition have the smallest optimal probability of being unambiguously discriminated. In this case, the probability of success becomes $1 - |\lambda_1 - \lambda_2|$.

A nontrivial relation between $|\gamma|$ and λ_1 is obtained from the intervals defined by $|\beta|$ and $\min\{\sqrt{p_1/p_2}, \sqrt{p_2/p_1}\}$ in Eq. (16). Figure 2(a) shows regions of the $(|\gamma|^2, \lambda_1)$ plane, where $0 \leqslant |\beta| \leqslant \min\{\sqrt{p_1/p_2}, \sqrt{p_2/p_1}\}$ (gray) and where $\min\{\sqrt{p_1/p_2}, \sqrt{p_2/p_1}\} \leqslant |\beta| \leqslant 1$ (black $p_1 \leqslant p_2$ and white $p_1 \geqslant p_2$). It is worth emphasizing that in the gray area of Fig. 2(a) both states $|\beta_1\rangle$ and $|\beta_2\rangle$ can be unambiguously discriminated, whereas in the white and black zones only the state associated with the higher probability p_1 or p_2 can be discriminated. Specifically, in the white (black) area, only $|\beta_1\rangle$ ($|\beta_2\rangle$) can be discriminated. In Fig. 2(b), we plot in degradation black-gray-white the optimal success probability (16) as a function of $|\gamma|^2$ and λ_1. In Fig. 3, we show the Eq. (16) probability (solid lines) as functions of $|\gamma|^2$ for different values of λ_1. Notice that p_s as a function of $|\gamma|^2$ is symmetric with respect to λ_1 and λ_2 and the minimal values are just at $|\gamma| = \sqrt{\lambda_1}$.

On the other hand, the two states of the $|\gamma|$ decomposition could be recognized tolerating an error. In this case, the strategy of discriminating them with minimum error leads to the Helstrom limit [11,18]:

$$p_e = \tfrac{1}{2}(1 - \sqrt{1 - 4p_1 p_2|\langle\beta_1|\beta_2\rangle|^2}). \tag{17}$$

Inserting into this expression p_1 and p_2 from Eqs. (8) and $|\langle\beta_1|\beta_2\rangle|$ from Eq. (10), we obtain the probability of

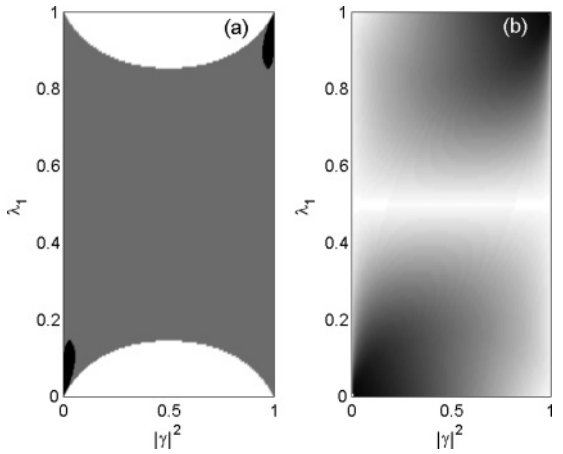

FIG. 2. (a) Regions of the $(|\gamma|^2,\lambda_1)$ plane, where $0 \leqslant |\beta| \leqslant \min\{\sqrt{p_1/p_2},\sqrt{p_2/p_1}\}$ (gray) and where $\min\{\sqrt{p_1/p_2},\sqrt{p_2/p_1}\} \leqslant |\beta| \leqslant 1$ (black and white); (b) the p_s optimal probability as a function of $|\gamma|^2$ and λ_1. Black stands for $p_s = 0$, white means $p_s = 1$, and the gray degradation goes linearly from 0 to 1.

discriminating with minimum error the $|\gamma|$-decomposition states,

$$p_e = \frac{1}{2}\left(1-\sqrt{1-4\frac{\lambda_1\lambda_2|\lambda_1-\lambda_2|^2|\gamma|^2(1-|\gamma|^2)}{[\lambda_1+(\lambda_2-\lambda_1)|\gamma|^2]^2}}\right). \quad (18)$$

This probability reaches its smallest value, 0, in the extreme values $|\gamma| = 0$ and $|\gamma| = 1$, which correspond to the spectral decomposition, whereas it has the highest value just for $|\gamma| = \sqrt{\lambda_1}$, which corresponds to the balanced decomposition. Thus the states belonging to the balanced decomposition have the highest probability of discriminating them with minimum error and this is $\frac{1}{2}(1-\sqrt{1-|\lambda_1-\lambda_2|^2})$. In Fig. 3, we show the Eq. (18) probability (dotted lines) as functions of $|\gamma|^2$ for different values of λ_1. We can see that it has its maximal values for the states of the balanced decomposition ($|\gamma| = \sqrt{\lambda_1}$) and has the minimum value, 0, for the states of the spectral one ($|\gamma| = 0, 1$).

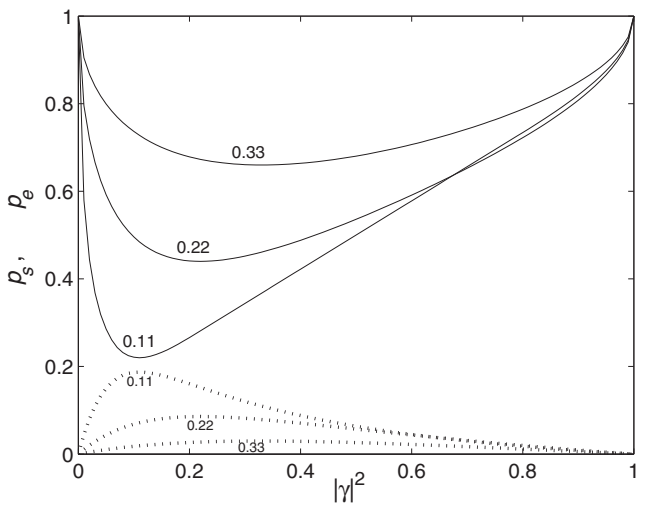

FIG. 3. Optimal success probability p_s (solid lines) and optimal probability of minimum-error p_e (dotted lines) as functions of $|\gamma|^2$ for different values of λ_1, say 0.11, 0.22, and 0.33. The respective values of λ_1 are indicated for each of the curves.

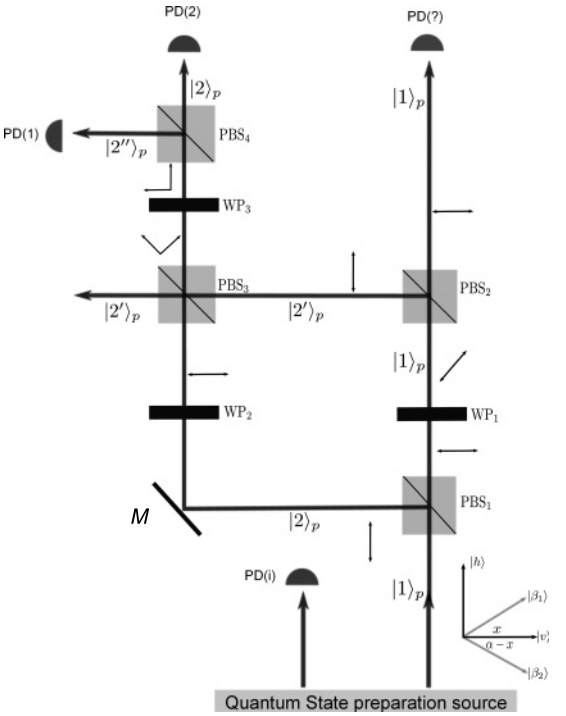

FIG. 4. Experimental setup sketch used to discriminate conclusively two nonorthogonal quantum states with different *a priori* probabilities. We have denoted by WP the wave plate, by PBS the polarizing beam splitter, by *M* the mirror, and by PD the single-photon photodiode detectors.

V. EXPERIMENTAL SCHEME FOR OPTIMAL UQSD

For the unambiguous states discrimination protocol, we propose a modified version of the experimental setup sketched in Ref. [9]; see Fig. 4. In that reference, they implement an optical setup for discriminating unambiguously two nonorthogonal states with equal *a priori* probabilities. Our modification allows implementing that optical setup for discriminating unambiguously two nonorthogonal states with either equal or different *a priori* probabilities in an optimal way.

We denote by $|h\rangle$ the horizontal and by $|v\rangle$ the vertical polarization photon states. For increasing the Hilbert space, we consider an ancillary system, which consists of a set of four orthogonal effective distinguishable propagation paths denoted by the states $|1\rangle_p$, $|2\rangle_p$, $|2'\rangle_p$, and $|2''\rangle_p$, as shown in Fig. 4.

We assume that the two nonorthogonal possible states $|\beta_i\rangle$, each one having *a priori* probability p_i, enter asymmetrically with respect to the horizontal polarization photon state $|h\rangle$, specifically,

$$|\beta_1\rangle = \cos x|h\rangle + \sin x|v\rangle,$$
$$|\beta_2\rangle = \cos(\alpha - x)|h\rangle - \sin(\alpha - x)|v\rangle.$$

A PBS transmits the horizontal polarization and reflects the vertical one, introducing in addition a phase of $\pi/2$. Thus,

after the photon passes through the PBS1, the $|\beta_i\rangle|1\rangle_p$ states are transformed as follows:

$$|\beta_1\rangle|1\rangle_p \to \cos x|h\rangle|1\rangle_p + i\ \sin x|v\rangle|2\rangle_p,$$
$$|\beta_2\rangle|1\rangle_p \to \cos(\alpha - x)|h\rangle|1\rangle_p - i\ \sin(\alpha - x)|v\rangle|2\rangle_p.$$

We consider that the WP1 rotates the photon polarization state $|h\rangle$ an angle ϕ, and the WP2 rotates it φ. Therefore, the states change to

$$\begin{aligned}|\beta_1\rangle|1\rangle_p \to{}& \cos x(\cos\phi|h\rangle + \sin\phi|v\rangle)|1\rangle_p \\ &+ i\sin x(\sin\varphi|h\rangle - \cos\varphi|v\rangle)|2\rangle_p, \\ |\beta_2\rangle|1\rangle_p \to{}& \cos(\alpha - x)(\cos\phi|h\rangle + \sin\phi|v\rangle)|1\rangle_p \\ &- i\sin(\alpha - x)(\sin\varphi|h\rangle - \cos\varphi|v\rangle)|2\rangle_p.\end{aligned}$$

The unitary effect of the PBS2 on the previous states is

$$\begin{aligned}|\beta_1\rangle|1\rangle_p \to{}& \cos x(\cos\phi|h\rangle|1\rangle_p + i\ \sin\phi|v\rangle|2'\rangle_p) \\ &+i\ \sin x(\sin\varphi|h\rangle - \cos\varphi|v\rangle)|2\rangle_p, \\ |\beta_2\rangle|1\rangle_p \to{}& \cos(\alpha - x)(\cos\phi|h\rangle|1\rangle_p + i\ \sin\phi|v\rangle|2'\rangle_p) \\ &-i\ \sin(\alpha - x)(\sin\varphi|h\rangle - \cos\varphi|v\rangle)|2\rangle_p.\end{aligned}$$

Meanwhile, the unitary effect of the PBS3 transforms them as follows:

$$\begin{aligned}|\beta_1\rangle|1\rangle_p \to{}& \cos x\ \cos\phi|h\rangle|1\rangle_p + i\sqrt{q_{s1}}|\eta_1\rangle|2\rangle_p \\ &+ \sin x\cos\varphi|v\rangle|2'\rangle_p, \\ |\beta_2\rangle|1\rangle_p \to{}& \cos(\alpha - x)\cos\phi|h\rangle|1\rangle_p - i\sqrt{q_{s2}}|\eta_2\rangle|2\rangle_p \\ &- \sin(\alpha - x)\cos\varphi|v\rangle|2'\rangle_p,\end{aligned}$$

where we have defined the normalized states,

$$|\eta_1\rangle = \frac{\sin x\ \sin\varphi|h\rangle + i\ \cos x\ \sin\phi|v\rangle}{\sqrt{q_{s1}}}, \tag{19a}$$

$$|\eta_2\rangle = \frac{\sin(\alpha - x)\sin\varphi|h\rangle - i\ \cos(\alpha - x)\sin\phi|v\rangle}{\sqrt{q_{s2}}}, \tag{19b}$$

and the probabilities,

$$q_{s1} = \cos^2 x\ \sin^2\phi + \sin^2 x\ \sin^2\varphi,$$
$$q_{s2} = \cos^2(\alpha - x)\sin^2\phi + \sin^2(\alpha - x)\sin^2\varphi.$$

From Eqs. (19), we realize that conclusive discrimination can be performed if $|\eta_1\rangle$ and $|\eta_2\rangle$ are orthogonal. This requirement is satisfied when

$$\sin^2\phi = \tan x\ \tan(\alpha - x)\sin^2\varphi. \tag{20}$$

It is important to point out that the initial angles α and x are restricted in such a way that the right-hand side of Eq. (20) has to be higher than or equal to 0 and lower than or equal to 1. Specifically, it is satisfied for all ϕ and φ when $0 \leqslant x \leqslant \alpha$. Therefore, by considering satisfying the condition (20) and $0 \leqslant x \leqslant \alpha$, the conclusive discrimination of the nonorthogonal $|\beta_i\rangle$ states becomes just the discrimination between the two orthogonal polarizations $|\eta_1\rangle$ and $|\eta_2\rangle$ of the single photon in the path $|2\rangle_p$. Inserting the expression (20) into the probabilities q_{si} we find, as a function of x, the probability $p_s(x)$ of successfully discriminating the $|\beta_i\rangle$ states; this is

$$\begin{aligned}p_s(x) &= p_1 q_{s1} + p_2 q_{s2}, \\ &= \left[p_1\frac{\sin x}{\cos(\alpha - x)} + p_2\frac{\sin(\alpha - x)}{\cos x}\right]\sin\alpha\ \sin^2\varphi.\end{aligned} \tag{21}$$

The first term $p_1 q_{s1}$ corresponds to the probability of discriminating the $|\beta_1\rangle$ state and the second term for discriminating $|\beta_2\rangle$, without ambiguity. For $x = 0$ ($x = \alpha$), there is no probability of discriminating $|\beta_1\rangle$ ($|\beta_2\rangle$). For other values of x, both states can be discriminated with probabilities different from zero. We also can note that when the initial states $|\beta_i\rangle$ are prepared symmetrically ($x = \alpha/2$) with respect to the horizontal polarization, the probability (21) does not depend on the *a priori* probabilities p_1 and p_2. Therefore, the asymmetry is necessary for the optimization. Figure 5 shows $p_s(x)$ as a function of x for different values of α and p_1. Note that, depending on the values of α and p_1, the function $p_s(x)$ has its maximal value inside the interval or at one of the extreme values of x, say $x = 0$ if $p_1 < p_2$ or $x = \alpha$ if $p_1 > p_2$. From Eq. (21), one analytically finds that the optimal value of the total probability of success, $p_s(x)$, is in x such that

$$\cos x = \frac{\sqrt{p_2}\sin\alpha}{\sqrt{1 - 2\sqrt{p_1 p_2}\cos\alpha}},$$

and the maximal one becomes

$$p_{s,\max} = \begin{cases}(1 - 2\sqrt{p_1 p_2}\cos\alpha)\sin^2\varphi & \text{if} \quad 0 \leqslant \cos\alpha \leqslant \min\left\{\sqrt{\frac{p_1}{p_2}}, \sqrt{\frac{p_2}{p_1}}\right\}, \\ (1 - \cos^2\alpha)\max\{p_1, p_2\}\sin^2\varphi & \text{if} \quad \min\left\{\sqrt{\frac{p_1}{p_2}}, \sqrt{\frac{p_2}{p_1}}\right\} \leqslant \cos\alpha \leqslant 1,\end{cases} \tag{22}$$

which is just the well-known Jeager and Shimony formula (16) for $\varphi = \pm\pi/2$ (here $\cos\alpha = |\langle\beta_1|\beta_2\rangle|$) [21].

In this optimal case, the $|\eta_i\rangle$ states of Eqs. (19) become

$$|\eta_1\rangle = \cos\xi|h\rangle + \sin\xi|v\rangle, \tag{23a}$$

$$|\eta_2\rangle = -\sin\xi|h\rangle + \cos\xi|v\rangle, \tag{23b}$$

where

$$\cos\xi = \frac{\sqrt{p_1 - \sqrt{p_1 p_2}\cos\alpha}}{\sqrt{1 - 2\sqrt{p_1 p_2}\cos\alpha}}$$

when $0 \leqslant \cos\alpha \leqslant \min\{\sqrt{p_1/p_2}, \sqrt{p_1/p_2}\}$. When $\min\{\sqrt{p_1/p_2}, \sqrt{p_2/p_1}\} \leqslant \cos\alpha \leqslant 1$ and $p_1 < p_2$ the Eqs. (19) become

$$|\eta_1\rangle = i|v\rangle, \tag{24a}$$

$$|\eta_2\rangle = |h\rangle, \tag{24b}$$

or

$$|\eta_1\rangle = |h\rangle, \tag{25a}$$

$$|\eta_2\rangle = -i|v\rangle, \tag{25b}$$

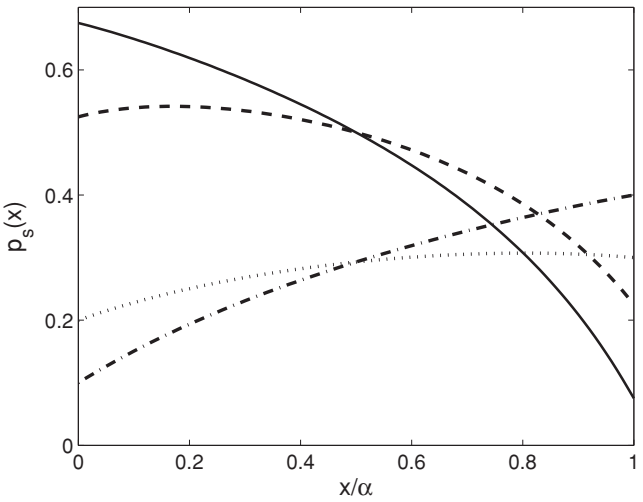

FIG. 5. Success probability $p_s(x)$ as functions of x for different values of α, and p_1, say $\alpha = \pi/3$ with $p_1 = 0.1$ (solid) and $p_1 = 0.3$ (dashes), $\alpha = \pi/4$ with $p_1 = 0.6$ (dots), and $p_1 = 0.8$ (dash-dot).

if $p_1 > p_2$. The WP3 (see Fig. 4) rotates the orthogonal photon polarized state (23) in such a way that $|\eta_1\rangle \to |v\rangle$ and $|\eta_2\rangle \to |h\rangle$. In this form, the PBS4 takes the orthogonal outcome polarization states into the detector PD(1) or PD(2) with optimal probability. When the process is optimized with respect to x and φ ($\varphi = \pm\pi/2$), there is no outcome through the path $|2'\rangle_p$ and so the inconclusive outcome through the path $|1\rangle_p$ is detected with minimal probability $1 - p_{s,\max}$ at the PD(?) photodetector. On the other hand, if $\min\{\sqrt{p_1/p_2}, \sqrt{p_1/p_2}\} \leqslant \cos\alpha \leqslant 1$, the $|\eta_i\rangle$ states coincide with the vertical and the horizonal polarization states, as can be seen from Eqs. (24) and (25); therefore, in this case the WP3 is not required.

Thus we have designed a physical scheme for discriminating conclusively and optimally two nonorthogonal states associated with different *a priori* probabilities. Therefore, this designed experimental setup allows one to discriminate desired $|\gamma|$-decomposition states of a two-rank mixed state.

VI. SUMMARY

In this paper, we have presented a physical test for the LI pure-state decomposition property of a rank-two mixed state.

We begin by proposing a protocol for preparing a qubit in two nonorthogonal states by starting from an entangled pure state. We show that the set of two nonorthogonal states can be chosen from a wide family of sets. We characterize by a complex parameter all the possible LI pure-state decompositions of a mixed state lying in a two-dimensional Hilbert space. The physical test consists of performing a process of recognition of one of the two linearly independent pure states that arise from a desired decomposition. We find that the two states associated with the balanced pure-state decomposition have the smallest probability of being conclusively discriminated, while in the nonconclusive scheme they have the highest probability of having an error. In addition, we designed an experimental scheme that allows one to discriminate conclusively and optimally two nonorthogonal states prepared with different *a priori* probabilities. We have proposed an experimental implementation for this linearly independent pure-state decomposition and UQSD test by using a one-photon polarization state generated in the process of spontaneous parametric down-conversion (SPDC) where the second single photon is considered for heralded detection.

For preparing the Eq. (3) and then the Eq. (5) state, the protocol described in Sec. II can be implemented with twin photons generated noncollinearly in a SPDC [22]. The (s) signal and (i) idler twin photons are generated noncollinearly by SPDC in the normalized state $|\Psi\rangle_{s,i} = \sqrt{\lambda_1}|h\rangle_s|h\rangle_i + \sqrt{\lambda_2}|v\rangle_s|v\rangle_i$. In this form, by ignoring the polarized state of the idler photon, we get the Eq. (5) state for the signal photon with $|\lambda_1\rangle = |h\rangle$ and $|\lambda_2\rangle = |v\rangle$. The experiment described in Ref. [22] was implemented by using a 351.1-nm single-mode Ar-ion laser pump with a 200-mW and 5-mm-thick β-BaB_2O_4 (BBO) crystal [23], cut for type-II phase matching, which allows a higher stability. Our proposed scheme for linearly independent pure-state decomposition and unambiguous quantum state discrimination could also be implemented with this setup.

ACKNOWLEDGMENTS

This work was supported by FONDECyT 1080535. M.A.-V. thanks CONICyT for financial support.

[1] M. A. Nielsen and I. L. Chuang, *Quantum Computation and Quantum Information* (Cambridge University Press, Cambridge, UK, 2000); N. M. Merming, *Quantum Computer Science* (Cambridge University Press, Cambridge, UK, 2007).
[2] C. Cohen-Tannoudji, B. Diu, and F. Laloë, *Quantum Mechanics* (Wiley, New York, 1977).
[3] L. Roa, A. Krügel, and C. Saavedra, Phys. Lett. A **366**, 563 (2007); L. Roa and G. A. Olivares-Renteria, Phys. Rev. A **73**, 062327 (2006).
[4] W. K. Wootters, Phys. Rev. Lett. **80**, 2245 (1998).
[5] M. Orszag, L. Roa, and R. Ramírez, Phys. Rev. A **48**, 4648 (1993); Opt. Commun. **86**, 147 (1991).
[6] A. Chefles, Phys. Lett. A **239**, 339 (1998).
[7] A. Peres, Phys. Lett. A **128**, 19 (1988).
[8] A. Chefles and S. M. Barnett, Phys. Lett. A **250**, 223 (1998).
[9] R. B. M. Clarke, A. Chefles, S. M. Barnett, and E. Riis, Phys. Rev. A **63**, 040305(R) (2001).
[10] L. Roa, J. C. Retamal, and C. Saavedra, Phys. Rev. A **66**, 012103 (2002).
[11] C. W. Helstrom, *Quantum Detection and Estimation Theory* (Academic, New York, 1976).
[12] M. Sasaki and O. Hirota, Phys. Rev. A **54**, 2728 (1996).
[13] R. B. M. Clarke, V. M. Kendon, A. Chefles, S. M. Barnett, E. Riis, and M. Sasaki, Phys. Rev. A **64**, 012303 (2001).

[14] L. Roa, C. Hermann-Avigliano, R. Salazar, and A. B. Klimov, Phys. Rev. A **84**, 014302 (2011).
[15] L. Roa, M. L. Ladrón de Guevara, and A. Delgado, Phys. Rev. A **81**, 034101 (2010).
[16] I. Sainz, L. Roa, and A. B. Klimov, Phys. Rev. A **81**, 052114 (2010).
[17] J. Wong, J. Math. Phys. **8**, 2039 (1967); H. C. Baker, Phys. Rev. A **30**, 773 (1984).
[18] S. M. Barnett and E. Riis, J. Mod. Opt. **44**, 1061 (1997).
[19] I. D. Ivanovic, Phys. Lett. A **123**, 257 (1987).
[20] D. Dieks, Phys. Lett. A **126**, 303 (1988).
[21] G. Jaeger and A. Shimony, Phys. Lett. A **197**, 83 (1995).
[22] F. A. Torres-Ruiz, J. Aguirre, A. Delgado, G. Lima, L. Neves, S. Pádua, L. Roa, and C. Saavedra, Phys. Rev. A **79**, 052113 (2009).
[23] W.-D. Cheng, J.-S. Huang, and J.-X. Lu, Phys. Rev. B **57**, 1527 (1998).